Role of network connectivity in intercellular calcium signaling

I.V. Dokukina [a,c], M.E. Gracheva [b], E.A. Grachev [c] and J.D. Gunton [a]

[a] *Department of Physics, Lehigh University, PA 18015, USA*

[b] *University of Illinois at Urbana-Champaign, Beckman Institute for Advanced Science and Technology, Urbana, IL 61801, USA*

[c] *Faculty of Physics, Moscow State University, Moscow, Russia*

Abstract

It is important to understand the coordinated performance of cells in tissue. One possible mechanism in this coordination involves intracellular Ca^{2+} signalling. The topology of intercellular connections in tissue should also play an important role in this process. It is most relevant for plane tissues, in which the interaction between cells is due to gap junctions (epithelium, blood vessels). We demonstrate the importance of the topology of intercellular connectivity by investigating the properties of a model of Ca^{2+} signaling for a small number of connected cells.

Key words: Calcium signaling, gap junction, intercellular, topology.
PACS: 02.60.Lj, 82.40.Bj, 87.15.Aa, 87.18.Pj

E-mail addresses of all authors:
Irina V. Dokukina: irina_g@mail.ru
Maria E. Gracheva: gracheva@uiuc.edu
Eugene A. Grachev: grace@cmp.phys.msu.su
James D. Gunton: jdg4@lehigh.edu

Corresponding author: Irina V. Dokukina. Permanent address: Moscow State University, Faculty of Physics, building 2, room 2-40a, Leninskie Gory, Moscow, 119992, Russian Federation. Phone: 7-(495)-939-4178. E-mail address: irina_g@mail.ru.

1 Introduction

Calcium ions (Ca^{2+}) are one of the universal regulators of various intra- and intercellular processes [1]. In the presence of connections between cells, when each cell is a piece of tissue, Ca^{2+} signal can be passed from cell to cell as intercellular Ca^{2+} wave [2]. The importance of intercellular Ca^{2+} signaling (among other secondary messengers) in the coordinated performance of cells in tissues is currently under investigation. These waves have been seen in a variety of cell types [3], [4], [5], [6]. Intercellular Ca^{2+} waves can be initiated by a focal mechanical, electrical, or hormonal stimulus. Often such waves travel from cell to cell in an oscillatory manner, thus forming periodic intercellular calcium waves [7], [8].

Intercellular Ca^{2+} signaling may occur through different pathways, for example through paracrine or junctional routes. In recent study [9] it was shown for astrocytes that propagation of intercellular Ca^{2+} waves in glia is essentially determined by both gap junctions between cells and paracrine signaling by ATP, other nucleotides and/or their metabolites. A detailed theoretical and experimental study of calcium oscillations in astrocytes doublets and linearly coupled triplets is given by Ullah et al. [10]. A model of intercellular calcium waves based on the action of calcium as a second messenger in paracrine signal transduction via calcium sensing receptor was proposed by Gracheva and Gunton [11] and extended for a linear chain of cells by Kepseu and Woafo [12].

Liver, blood vessels, brain and epithelium are very good examples of tissues in which cells are connected with each other by gap junctions. It was shown by experiments and modeling that mechanically stimulated intercellular Ca^{2+} waves in epithelial, glial and endothelial cells can result from the diffusion of inositol 1,4,5-trisphosphate (IP_3) through gap junctions [13], [14], [15]. Although Ca^{2+} can move through gap junctions, a cellular Ca^{2+} wave is the cellular response to a diffusing of IP_3, passing between cells via gap junctions and consequently participating in the release of Ca^{2+} ions from the intracellular stores. However, in contrast with these cell types, the amount of IP_3 diffusing through the gap junctions in connected hepatocytes is insufficient to induce a Ca^{2+} response [7], [16], [17], [18]. Thus, models based on the passive diffusion of IP_3 between adjacent cells through gap junctions [15] cannot account for apparent intercellular Ca^{2+} waves in hepatocytes. Hoefer [19] has proposed an alternative mechanism of intercellular calcium waves in hepatocytes, based on the diffusion of cytosolic calcium through gap junctions. Stochastic versions of both the [17] and [19] models are given by Gracheva et al. [20]. Clair et al. [16] have also shown that an agonist receptor gradient could be responsible for the apparent undirectional Ca^{2+} waves observed in multiplets or in perfused intact livers. In this case, the main factor influencing Ca^{2+} wave propagation

in hepatocytes is the cellular distribution of agonist receptors.

In addition, Tsaneva-Atanasova et al. [21] have shown for pancreatic acinar cells that intercellular calcium diffusion is necessary and sufficient to synchronize Ca^{2+} oscillations in neighboring cells, whereas the function of intercellular IP_3 diffusion is to provide the propagation of oscillating Ca^{2+} waves in tissue.

In all the above mentioned models the junctional permeability was chosen to be constant. However, since calcium ions can close gap junctions [22], [23], this would appear to pose an obstacle to the propagation of intercellular Ca^{2+} waves via gap junctions. Fortunately, this apparent paradox can be resolved by considering the temporal aspects of these responses. It is known that extended exposure to high concentrations of Ca^{2+} (> 10 μM) results in the closure of gap junctions [22], [23]. It also appears that physiological concentrations of Ca^{2+} can reversibly close gap junctions but this response takes about 30 s [24]. Thus, because Ca^{2+} waves propagate faster than the proposed closure times [25], the two possible intercellular messengers (Ca^{2+} and IP_3) [26], [27] can diffuse to adjacent cells to propagate the wave before Ca^{2+} closes the gap junctions. Therefore, it would seem that a more accurate description of the gap junction permeability requires taking into account its dependence on the cytosolic calcium concentration, rather than treating it as a constant as in the earlier models [15], [17], [19], [20].

We believe that an important issue in modeling intercellular calcium signaling is to account for the cellular topology of the tissue. As a rule, flat tissues are modeled in the form of a two-dimensional square grid [28], [29]. However, in reality, the structure of even flat tissues is significantly more complicated. Even small areas of tissue can exhibit different topological types of cell connections between each other [8], [27]. In addition, in the case of local stimulation in which only one cell (not the entire tissue) is stimulated, it is important to know which cell is stimulated (for the same structure of cell connections). Thus, the aim of our study is to investigate the relation between the topology of cellular connectivity in flat tissues and the corresponding intercellular calcium signaling.

Since gap junctions ensure a strict topology of intercellular connections, we take into account in our study only tissues in which cells are connected with each other by gap junctions and the main mechanism of intercellular Ca^{2+} wave propagation is a diffusion of a second messenger through these gap junctions. We do not exclude the possible influence of extracellular pathways on the intercellular calcium signaling. However, for the sake of clarity and simplicity, in this work we omit taking into account any second messenger diffusion through the extracellular matrix, which could be relevant, for example, in astrocytic networks [9]. In our model, we take into account only the diffusion of IP_3 through gap junctions as the main mechanism of Ca^{2+} wave propagation

in tissue [15], [21], [25]. Also we include in our model the dependence of gap junctional conductance on concentration of cytosolic Ca^{2+} [24].

2 Description of the model

We use the minimal model [30] as the basis of our model of intercellular Ca^{2+} signaling. In this model [30] the total constant entry of Ca^{2+} into the cytosol is $\nu_0+\nu_1\beta$. This includes the influx ν_0 from the extracellular medium and the IP_3-stimulated Ca^{2+} release $\nu_1\beta$ (β is the degree of saturation of the IP_3 receptor). It is more convenient for us to include in the model an explicit dependence on the IP_3 concentration in cell. Therefore we replace the IP_3-stimulated Ca^{2+} release $\nu_1\beta$ in [30] by its linear dependence on IP_3: $k_{inIP_3}IP_3$.

We also include gap junction tunneling between nearby cells. In order to model Ca^{2+} wave propagation the IP_3 stimulus (which mimics the local application of a stimulus) is applied only to the first cell. We model this IP_3 stimulus as a trapezoidal function of time for the first cell, which corresponds to external stimuli of different concentrations of agonists (J_{synt}). Modeling the agonist generated IP_3 concentration by trapezoids is more convenient numerically than, for example, using a square impulse. In addition, we add to the model a term describing the degradation of IP_3 [28] in each of the cells:

$$J_{deg} = \frac{V_p IP_3 k_p}{k_p + IP_3}, \tag{1}$$

where k_p is the half maximal rate of IP_3 degradation [28]. Without this term, the calcium levels reach unphysiological values in the asymptotic time limit [25]. The values of all the parameters are given in Table 1.

Lazrak et al. [24] have shown that during the fast increase of cytosolic Ca^{2+} concentration in each of the coupled adjacent cells (from 0.2 μM to 1 μM), the gap junctional conductance decreases from 100 % to 0 %. During the subsequent return of the level of cytosolic Ca^{2+} to its normal value (about 0.2 μM), the gap junctional conductance recovers with practically the same rate as its previous decrease (see Fig. 3 in [24]). This means that during each oscillation of cytosolic Ca^{2+} in one of two adjacent cells, the gap junctions between these cells are transiently closed. However, this closure does not occur instantaneously, but during an interval of about 30 s. Relying on these data (Fig. 3 in [24]), we model the fast changes in the gap junctional conductance γ_{ij} between adjacent cells i and j by the following function:

$$\gamma_{ij} = \frac{k_{ij}^n}{Ca_{cytMax(ij)}^n + k_G^n}, \tag{2}$$

where $Ca_{cytMax(ij)}$ is the larger of the two cytosolic calcium concentrations in cells i and j. Thus, $\gamma_{ij} = 1$ corresponds to a 100 % conductive gap junction between cell i and j. For other parameters see Table 1. The gap junctional conductance in Fig. 3 in [24] decreases very rapidly, even with a small increase of cytosolic Ca^{2+}. Therefore we choose $n = 5$ in the function (2) (see Fig. 1). The diffusion of IP_3 provides the mechanism of intercellular Ca^{2+} wave propagation in our model.

Thus, the evolution of our system is described by the following differential equations (cf. [30], for parameter values see Table 1):

$$\frac{dCa_{cyt(i)}}{dt} = k_{in} + k_{inIP_3} IP_{3(i)} - k_{out} Ca_{cyt(i)} +$$

$$+ (k_{pool} Ca_{pool(i)} + k_{rel} \frac{Ca^2_{pool(i)}}{K_1^2 + Ca^2_{pool(i)}} \frac{Ca^4_{cyt(i)}}{K_2^2 + Ca^4_{cyt(i)}}) - k_{serca} \frac{Ca^2_{cyt(i)}}{K_3^2 + Ca^2_{cyt(i)}}, \quad (3)$$

$$\frac{dCa_{pool(i)}}{dt} = k_{serca} \frac{Ca^2_{cyt(i)}}{K_3^2 + Ca^2_{cyt(i)}} -$$

$$- k_{rel} \frac{Ca^2_{pool(i)}}{K_1^2 + Ca^2_{pool(i)}} \frac{Ca^4_{cyt(i)}}{K_2^2 + Ca^4_{cyt(i)}} - k_{pool} Ca_{pool(i)}, \quad (4)$$

$$\frac{dIP_{3(i)}}{dt} = J_{synt} - J_{deg} + k_{gap} \gamma_{ij} (IP_{3(j)} - IP_{3(i)}) + k_{gap} \gamma_{ik} (IP_{3(k)} - IP_{3(i)}), \quad (5)$$

where the indices i, j and k denote the cell number, and k_{gap} is the coefficient of gap junctional communication for IP_3 (see Table 1).

The case in which the index pairs $(ijk) = (120) = (210)$ with $k_{13} = k_{23} = 0$ corresponds to just two coupled cells. The case in which $(ijk) = (100)$, $Ca_{cytMax(ij)} = Ca_{cyt(1)}$ and all junctional coefficients are equal to zero corresponds to just one cell. This is equivalent to equations for intracellular Ca^{2+} signaling. It is also worth noting that in the case of index pairs $(ijk) = (123) = (213) = (312)$ there are three possible different configurations of three coupled cells. If $k_{13} = 0$, we have a one-dimensional chain of cells, with the first cell interacting only with the second cell, the second cell interacting with both the first and third cells and the third cell interacting only with the second cell (see Fig. 2 A). The same linear chain with other orderings of the cells is shown in Fig. 2 B. If none of the junctional coefficients vanish, each cell interacts with two other cells (see Fig. 2 C). The right side of Fig. 2 shows graphs that correspond to these three configurations.

The system can be easily generalized to the case of more than three cells. For example, all the configurations in two dimensions of four coupled cells are shown in Fig. 3. All these are biologically realistic in two dimensions. Examples of real cellular configurations in vitro are shown in Fig. 1 and 2 in [27] and Fig. 9 and 11 in [8]. The system of cells 1, 2, 3, 7 in Fig. 1a in [27] (if

the rest of the cells are removed) corresponds to the topological configuration in Fig. 3 A (cell 3 or 7 should be stimulated) and 3 B (cell 1 or 2 should be stimulated) in our study. The system of cells 1, 2, 5, 7 in Fig. 1a in [27] (if the rest of the cells are removed) corresponds to the topological configuration in Fig. 3 C (cell 5 should be stimulated), 3 D (cell 2 or 7 should be stimulated) and 3 E (cell 1 should be stimulated) in our study. The system of cells 1, 3, 5, 7 in Fig. 1a in [27] (if the rest of the cells are removed) corresponds to the topological configuration in Fig. 3 F (cell 1 should be stimulated) and 3 G (cell 3, 5 or 7 should be stimulated) and the system of cells in Fig. 9 in [8] corresponds to the topological configuration in Fig. 3 F (cell B should be stimulated) and 3 G (cell A, C or D should be stimulated) in our study. The systems of cells in Fig. 1c and Fig. 2 in [27] and in Fig. 11 in [8] correspond to the topological configuration in Fig. 3 I and 3 J in the present paper. Finally, we believe that it is possible to extract the configuration shown in Fig. 3 H from a variety of cellular tissues.

3 Results

We first consider the case of two cells (see Fig. 4). We apply to the first cell a trapezoid impulse of IP_3 from 0 s to 14 s, with an amplitude of 4 μM. Some IP_3 from this impulse dissociates as J_{deg} (eq. (1)). The remainder of IP_3 diffuses into the second cell through gap junctions. The concentration of IP_3, which is received as the result of all these processes in the first cell, is shown on Fig. 4 ($IP_{3(1)}$ from 0 s to 14 s). The concentration of IP_3 which diffused into the second cell as the result of diffusion through gap junctions from the first cell is shown in Fig. 4 ($IP_{3(2)}$ from 0 s to 14 s). At the end of external stimulation of a cell by the agonist, the concentration of IP_3 in the cytosol falls rapidly to almost zero (see $IP_{3(1)}$, $t = 14$ s in Fig. 4). The increase of IP_3 concentration in the first cell after that (see $IP_{3(1)}$, $t > 14$ s in Fig. 4) occurs because of the feedback between cells. The change of IP_3 in both cells occurs in this period by large advances, rather than smoothly. This is connected with the fact that the gap junctional conductance between cells is changed according to γ_{ij} (eq. (2)), rather than remaining constant all the time. Thus, as gap junctions are completely closed at a high concentration of cytosolic Ca^{2+} in any two cells, the diffusion of IP_3 through them temporarily ceases.

Cytosolic Ca^{2+} oscillations in the model cell occur at concentrations of IP_3 about 1 μM. This concentration of IP_3 is the required level in the second cell that occurs at a time later than in the first cell. Therefore, the cytosolic Ca^{2+} oscillations in the second cell arise after a certain time delay (see Fig. 5). We find in our model an inverse dependence of this time delay on the amplitude of the impulse of IP_3 which is applied to the first cell (see Fig. 5).

For more than two connected cells, our model shows that the propagation of calcium waves depends on the spatial configuration of cells; this may be interpreted as the first indication of heterogeneity in intercellular Ca^{2+} wave propagation. There are three possible configurations of interactions between three cells (see Fig. 2). If the location of the two neighboring cells is symmetric with respect to the first cell (Fig. 2 B, C), than one can see similar oscillations in both the second and third cells, following an initial delay of about 2 s from the onset of oscillations in the first cell. In the case of a linear chain (Fig. 2 A), there is a difference in the calcium oscillations in the second and third cells. There is not only a delay time between the onset of calcium oscillations in the first and second cells, but also between the second and third cells (both delay times are about 2.5 s). The value of this delay time slightly differs from that found in [25], [28]. This is due to the different choice of parameter values in the two studies.

We also briefly describe the results for the case of four connected cells. The results for all configurations of four cells are summarized in Tables 2 – 4. We note that we study only in-plane (two-dimensional) cell configurations. It is possible to distinguish five different configurations of four cells on a plane. However, for the same topological configuration of cells, the Ca^{2+} signaling greatly depends on which cell in the structure is stimulated. Taking into account this fact, we identify ten cell configurations. As in the case of three cells, the dynamics of Ca^{2+} in cells symmetrically positioned with respect to the stimulated cell is identical; for example, see configurations "A", "B", "C", "E", "F", "G" and "H" in Fig. 3. This holds when all the cells in these configurations are indistinguishable. Also, this assumption allows us to study the dependence of the intercellular Ca^{2+} signaling only on the topology of the cell to cell connections in a given cell configuration.

We now discuss the key features of signaling in four cells configurations. For example, in the case of configuration "H" (Fig. 3 H) the first cell has two connections with adjacent cells (there are four connections between cells altogether) and we find very good calcium wave propagation between cells (see Fig. 6). Also, the dynamics of Ca^{2+} in cells 2 and 3, which are positioned symmetrically with respect to the stimulated cell 1, is the same (see Tables 2 and 4, Fig. 6). The delay time between the onset of Ca^{2+} oscillations in the stimulated cell and the beginning of oscillations in all other cells in the configuration depends on the ordering number of neighbors of a given cell. In the case of a direct connection with the first simulated cell (first order neighbors) the delay time varies from 2 s to 5 s (see Table 3). For example, in configuration "I" cell 2 is the first order neighbor of cell 1. For a second order neighbor, there is one additional cell between the stimulated cell and a given cell. For example, in configuration "I" cell 3 is the second order neighbor for cell 1. For second order neighbors, the time delay for onset of Ca^{2+} oscillation varies from 4 s to 9.5 s; this is larger then in the case of the first order neighbors (see

Table 3). In addition, for cells next to the stimulated cell there is a difference in response depending on the presence or absence of connections with other second order neighbors (compare cell 3 and cell 4 in configurations "C" and "G", Tables 2 – 4). This suggests a heterogeneity in the Ca^{2+} response in these cell networks. Of course, larger cell networks would have to be studied to strengthen this conclusion. For in-plane configurations of four cells there is only one neighbor of third order which is present in configuration "I". For the given parameters there are no oscillations in cell 4 of configuration "I", as indicated in Tables 2 – 4 and Fig. 8.

Thus, each cell configuration can be characterized by a definite set of neighbors of each order; moreover, the propagation of intercellular Ca^{2+} waves for each configuration depends on this set. According to the set of neighbors, all cell configurations can be divided into four classes:

- one neighbor of first order, one neighbor of second order, one neighbor of third order (configuration "I");
- one neighbor of first order, two neighbors of second order (configurations "C", "G");
- two neighbors of first order, one neighbor of second order (configurations "A", "D", "H", "J");
- three neighbors of first order (configurations "B", "E", "F").

A fast decline of intercellular Ca^{2+} waves is characteristic of the first two classes, whereas a steady expansion of intercellular Ca^{2+} waves is characteristic of the last two classes (see Tables 2 – 4). For example, in the case of configuration "C" (Fig. 3 C) the first cell has only one connection with another cell (there are four connections between all cells, as in "H") and this results in a decreased range of the calcium wave propagation from the first cell (see Fig. 6). There is an even stronger decrease in the range of wave propagation in the case of configuration "I", which is a linear chain of four cells (see Fig. 8).

We now consider some interesting configurations of four cells in more detail. Configuration "C" (Fig. 3 C) belongs to the second class of configurations. In this configuration the cytosolic Ca^{2+} displays the typical dynamics of this class, i.e., prolonged high-frequency Ca_{cyt} oscillations in the first cell and shorter Ca_{cyt} oscillations with lower frequency in the other cells. Cells 3 and 4 are equally spaced with respect to the first cell in configuration "C"; therefore their cytosolic Ca^{2+} dynamics is identical. At the same time the total intensity of oscillations decreases with the distance from the first cell. Configuration "D" (Fig. 3 D) belongs to the third class in our classification. The topological difference between configurations "D" and "J" consists in the presence (configuration "D") and absence (configuration "J") of a connection between cells 2 and 3. This difference is manifested in Ca^{2+} dynamics, primar-

ily through small temporary distinctions (see Tables 3 and 4) and also in a weaker response in cell 2 in configuration "D", as compared with configuration "J" (see Table 4). This is connected with the fact that cell 2 in configuration "D" exchanges IP_3 with cell 3 in addition to cell 1, whereas there is no such exchange in configuration "J". Note that although in configuration "D", the disposition of cells 2 and 3 in the absence of cell 4 is symmetrical relative to cell 1 (Fig. 3 D), the cytosolic Ca^{2+} dynamics in cells 2 and 3 is different (see Fig. 6). This is the result of the fact that cell 4 is an additional neighbor of cell 3, and an additional exchange of IP_3 between these two cells takes place. That exchange decreases the duration of oscillations in cell 3 in comparison with cell 2 in configuration "D" (see Fig. 6).

We find one more interesting regularity in the case of different configurations for four cells. We calculate the sum of the durations of Ca^{2+} oscillations (last column in Table 2) and the sum of the number of peaks of Ca^{2+} oscillations (last column in Table 4) in all four cells, for each configuration. Then we divide this total number of Ca^{2+} oscillations by the corresponding total duration of Ca^{2+} oscillations for each configuration and determine the mean frequency of oscillation for each configuration (Fig. 7). There is obviously a good correlation of this mean frequency with the classes of configurations described above. In other words, we find a correlation of each configuration class with a mean frequency for this class. This regularity allows us to conclude that the topology of the graph of intercellular connections has a more important influence on intercellular Ca^{2+} signaling than one might think at first glance.

We find that a variable gap junctional conductance can significantly influence the range of intercellular Ca^{2+} wave propagation. This is most clear for the chain of four cells (configuration "I", Fig. 3 I). If the gap junctional conductance is described by γ_{ij} (eq. (2)), Ca^{2+} oscillations take place only in cells 1, 2 and 3, but the Ca^{2+} wave does not reach cell 4 (Fig. 8). If the gap junctional conductance is constant and independent of Ca_{cyt} ($\gamma_{ij} = 1$), Ca^{2+} oscillations take place in all four cells of configuration "I" (Fig. 9). Therefore, even a brief closure of the gap junctions between cells has a strong effect on the propagation of intercellular Ca^{2+} waves.

We also consider the effect of varying the parameter k_G on the range of intercellular Ca^{2+} wave propagation. If one increases k_G, the gap junctional conductance γ_{ij} decreases. For configuration "I" with $k_G = 0.5$ μM, such a decrease of γ_{ij} results in an abrupt limitation of intercellular Ca^{2+} wave propagation. In this case, Ca^{2+} oscillations take place only during the first four seconds in the cell 1 of configuration "I", whereas in the other three cells there is only a negligible increase in cytosolic Ca^{2+} above its baseline value. If one decreases k_G, the gap junctional conductance γ_{ij} increases. For configuration "I" with $k_G = 0.3$ μM the corresponding increase in γ_{ij} results in an increase in the range of Ca^{2+} waves and higher frequency oscillations similar

to $\gamma_{ij} = 1$ at $k_G = 0.4$ μM (Fig. 9).

Finally, we find the following results for all the configurations. First (denoted as A below), with a constant gap junctional conductance ($\gamma_{ij} = 1$), the number of Ca^{2+} oscillations and their total duration increase, in contrast to the case with a variable $\gamma_{ij}(Ca_{cyt})$. Second (denoted as B below), several things remain the same whether or not the gap junction conductance varies with concentration. These include the response of symmetrically positioned cells, the general dependence of frequency and duration of Ca^{2+} oscillations in a cell on the number of its direct neighbors, and the relation between the time delays from the onset of oscillations in the first cell to the first oscillations in the other cells of the configuration.

The above-mentioned features are the consequence of IP_3 diffusion through the gap junctions. At the same time a variable gap junctional conductance influences only the absolute (rather than relative) values of IP_3. Thus, independently of whether there is a variable or constant gap junctional conductance, the qualitative dynamics of cytosolic Ca^{2+} during intercellular signaling for different topological configurations of cellular connections remain the same. This conclusion remains true if a different model of intracellular Ca^{2+} is used. Thus, the topology of cellular connections determines the signaling.

The first features (A) described above are the consequence of the different absolute values of IP_3 which are acquired by each cell in configurations with open and closed gap junctions. In the case of the features (B), it is not important how much IP_3 has arrived in a cell, since these are relative characteristics, and only the relative amount of IP_3 which moves between neighboring cells is important. For example, it is important whether the neighboring cells obtained equal amounts of IP_3 or not; if not, the difference in the amounts is important. Thus features (A) are absolute characteristics of the oscillations, and are determined by the behavior of the gap junctions, whereas features (B) are relative characteristics of the values in cells (of a given configuration) with respect to each other and are determined by the topological structure.

Next, we plot in Fig. 10, the same diagram as in Fig. 7, but for the case of $\gamma_{ij} = 1$. We find that we can distinguish only the first ("I") and the fourth ("B", "E", "F") configuration classes, but we cannot distinguish between the second or third classes in our configuration classification. To conclude, a variable gap junctional conductance has a modulating influence on intercellular Ca^{2+} signaling by reinforcing the role of the cellular connection topology, but leaves the qualitative aspects unchanged.

We have also considered Ca^{2+} diffusion through the gap junctions between cells, in addition to IP_3 diffusion between cells. We thus added an exchange term to eq. (3) in the form $k_{gap}\gamma_{ij}(Ca_{cyt(j)} - Ca_{cyt(i)})$, similar to eq. (5). The

results we obtain allow us to conclude that there are two separate mechanisms involved in intercellular signaling. First, IP_3 diffusion provides the mechanism for calcium wave propagation between cells, as was proposed in [28]. Second, the diffusion of Ca^{2+}, is necessary (in addition to IP_3 diffusion), to synchronize the oscillations among the neighboring cells. Similar conclusions were drawn by Tsaneva-Atanasova et al. [21], which are in complete agreement with this work.

4 Conclusion

Intercellular Ca^{2+} signaling is a complex and nonlinear process; its mechanism depends on the kind of tissue and the method used to stimulate the cells. In this work we study only plane tissues, cells of which are connected to each other by gap junctions, such as epithelium and blood vessels. We suggest that the diffusion of IP_3 through gap junctions is the main mechanism for intercellular Ca^{2+} wave propagation in such tissues. That is, we consider intercellular topological structures which are common to epithelium and endothelial tissues, but we do not model the details of the intracellular signaling specific to these cell types.

The intercellular Ca^{2+} wave propagation in airway epithelial cell cultures arises as the result of mechanical stimulation of a single cell in the tissue [25]. The front of this wave is heterogeneous in different directions; thus one can observe many kinds of "branches", "paws" and so on, as well as an oblongness of the front on a whole in some directions [25]. The reasons for such a heterogeneous wave propagation might include both the heterogeneity of the tissue structure (for example, the different number of gap junctions in the boundaries between adjacent cells, the different number of neighbors for each cell, the different shape of cells and so on), and the internal heterogeneity of the cellular structure (I.V.Dokukina, M.E.Gracheva, E.A.Grachev - unpublished results). In the current study we show that different numbers of neighbors results in a heterogeneity of intercellular Ca^{2+} wave propagation, while varying the gap junctional conductance amplifies this influence.

We believe that the topology of intercellular connections in tissue has an essential influence on Ca^{2+} signaling. We demonstrate this influence for the case of a small (three of four) number of cells, using the minimal model [30] for the description of intracellular processes. In addition, we take into account the dependence of the gap junctional conductance on the cellular concentration of cytosolic Ca^{2+}. Even in the simplest case of three cells we find differences in Ca^{2+} signaling between the linear chain of three cells (Fig. 2 A) and the closed chain in which each cell is connected to its adjacent cells (Fig. 2 C). We find a stronger influence of the topological structure of intercellular connections on

Ca^{2+} signaling for different configurations of four cells. We classify all possible plane configurations of four cells in four different categories, depending on the number of neighbors of a definite order. We find that the type of intercellular Ca^{2+} signaling in each configuration depends on the class of this configuration. Furthermore we find that by knowing the mean frequency of Ca^{2+} oscillations in any configuration, it is possible to refer this configuration to one of the four categories.

Our results suggest that during any investigations of intercellular Ca^{2+} signaling in a particular tissue, it is necessary to pay attention to the possible influence of the topology of cellular connections. This is most important for small pieces of tissue, because in this case the influence of topology is most evident. Note that we consider only two-dimensional configurations of cells in this paper. However, it would be interesting to consider the role of topological structure in three-dimensional tissues, which is a subject of our future research. Also, Tsaneva-Atanasova et al. [21] have shown that an analysis of the point-oscillator model is insufficient to determine which kinds of oscillations will appear in clusters of pancreatic acinar cells with realistic geometries. They also find that geometrical factors play a crucial role in both intra- and intercellular Ca^{2+} signaling. Therefore, it is important to carry out a study of spatially distributed models of the most interesting topological configurations of cellular connections.

While modeling the intercellular calcium signaling it is necessary to recognize that the transition from one cell to tissue is not a simple quantitative conversion. It is not a transition from one cell to a chain of cells or some grid of cells; rather, it is a more complex transition defined by the topology of tissue. We have shown that the dynamics of tissue in small areas (and also in larger regions – I.V. Dokukina, A.A. Tsukanov, M.E. Gracheva, E.A. Grachev, unpublished results) is defined not by a chain or grid of cells, but by the topology of the connection graph of cells with each other. It is possible to judge the tissue topology from the dynamics of signaling; in turn, the tissue topology can change the intercellular signaling dynamics, enforcing its own rhythm. Thus, the intercellular dynamics of calcium and the corresponding topology of cell connections form an unbroken, complete system.

5 Acknowledgments

This research was supported in part by grants from the National Science Foundation (DMR0302598), and the G. Harold and Leila Y. Mathers Charitable Foundation.

References

[1] M.J. Berridge, The biology and medicine of calcium signaling, Mol. Cell. Endocrinol. 98 (1994) 119-124.

[2] M.J. Berridge, M.D. Bootman, P. Lipp, Calcium - life and death signal, Nature 395 (1998) 645-648.

[3] S. Boitano, E.R. Dirksen, M.J. Sanderson, Intercellular propagation of calcium waves mediated by inositol trisphosphate, Science 258 (1992) 292-295.

[4] P. Loessberg-Stauffer, H. Zhao, K. Luby-Phelps, R.L. Moss, R.A. Star, S. Muallem, Gap junction communication modulates Ca^{2+} oscillations and enzyme secretion in pancreatic acini, J. Biol. Chem. 268 (1993) 19769-19775.

[5] A.H. Cornell-Bell, S.M. Finkbeiner, M.S. Cooper, S.J. Smith, Glutamate induces calcium waves in cultured astrocytes: long range glial signalling, Science 247 (1990) 470-473.

[6] J.W. Dani, A. Chernjavsky, S.J. Smith, Neuronal activity triggers calcium waves in hippocampal astrocyte networks, Neuron 8 (1992) 429-440.

[7] C. Clair, C. Chalumeau, T. Tordjmann, J. Poggioli, C. Erneux, G. Dupont, L. Combettes, Investigation of the roles of Ca^{2+} and $InsP_3$ diffusion in the coordination of Ca^{2+} signals between connected hepatocytes, J. Cell Sci. 114 (2001) 1999-2007.

[8] J.H. Evans, M.J. Sanderson, Intracellular calcium oscillations induced by ATP in airway epithelial cells, Am. J. Physiol. 277 (Lung Cell. Mol. Physiol. 21) (1999) L30-L41.

[9] D.A. Iacobas, S.O. Suadicani, D.C. Spray, E. Scemes, A stochastic two-dimensional model of intercellular Ca^{2+} wave spread in glia, Biophys. J. 90 (2006) 24-41.

[10] G. Ullah, P. Jung, A.H. Cornell-Bell, Anti-phase calcium oscillations in astrocytes via inositol (1,4,5)-trisphosphate regeneration, Cell Calcium 39 (2006) 197208.

[11] M.E. Gracheva, J.D. Gunton, Intercellular communication via intracellular calcium oscillations, J. Theor. Biol. 221 (2003) 513-518.

[12] W.D. Kepseu, P. Woafo, Intercellular waves propagation in an array of cells coupled through paracrine signaling: a computer simulation study, Phys. Rev. E 73 (2006) 041912.1-041912.7.

[13] L. Leybaert, K. Paemeleire, A. Strahonja, M.J. Sanderson, Inositol trisphosphate dependent intercellular calcium signaling in and between astrocytes and endothelial cells, Glia 24 (1998) 398-407.

[14] M.J. Sanderson, A.C. Charles, S. Boitano, E.R. Dirksen, Mechanisms and function of intercellular Ca^{2+} waves, Mol. Cell. Endocrinol. 98 (1994) 173-187.

[15] J. Sneyd, M. Wilkins, A. Strahonja, M.J. Sanderson, Calcium waves and oscillations driven by an intercellular gradient of inositol (1,4,5)-trisphosphate, Biophys. Chem. 72 (1998) 101-109.

[16] C. Clair, D. Tran, S. Boucherie, M. Claret, T. Tordjmann, L. Combettes, Hormone receptor gradients supporting directional Ca^{2+} signals: direct evidence in rat hepatocytes, J. Hepatol. 39 (2003) 489-495.

[17] G. Dupont, T. Tordjmann, C. Clair, S. Swillens, M. Claret, L. Combettes, Mechanism of receptor-oriented intercellular calcium wave propagation in hepatocytes, FASEB J. 14 (2000) 279-289.

[18] T. Tordjmann, B. Berthon, M. Claret, L. Combettes, Coordinated intercellular calcium waves induced by noradrenaline in rat hepatocytes: dual control by gap junction permeability and agonist, EMBO J. 16 (1997) 5398-5407.

[19] T. Hoefer, Model of intercellular calcium oscillations in hepatocytes: synchronization of heterogeneous cells, Biophys. J. 77 (1999) 1244-1256.

[20] M.E. Gracheva, R. Toral, J.D. Gunton, Stochastic effects in intercellular calcium spiking in hepatocytes, J. Theor. Biol. 212 (2001) 111-125.

[21] K. Tsaneva-Atanasova, D.I. Yule, J. Sneyd, Calcium oscillations in a triplet of pancreatic acinar cells, Biophys. J. 88 (2005) 1535-1551.

[22] M.V.L. Bennett, V.K. Verselis, Biophysics of gap junctions, Semin. Cell. Biol. 3 (1992) 29-47.

[23] J.C. Saez, V.M. Berthoud, A.P. Moreno, D.C. Spray, Gap junctions. Multiplicity of controls in differentiated and undifferentiated cells and possible functional implications, In: S. Shenolikar, A.C. Nairn, (eds). Advances in second messenger and phosphoprotein research, Raven Press. New York. 27 (1993) 163-198.

[24] A. Lazrak, A. Peres, S. Giovannardi, C. Peracchia, Ca-mediated and independent effects of arachidonic acid on gap junctions and Ca-independent effects of oleic acid and halothane, Biophys. J. 67 (1994) 1052-1059.

[25] M.J. Sanderson, A.C. Charles, E.R. Dirksen, Mechanical stimulation and intercellular communication increases intracellular Ca^{2+} in epithelial cells, Cell regulation 1 (1990) 585-596.

[26] J.C. Saez, J.A. Connor, D.C. Spray, V.L. Bennett, Hepatocyte gap junctions are permeable to the second messenger, inositol 1,4,5-trisphosphate, and to calcium ions, Proc. Natl. Acad. Sci. USA 86 (1989) 2708-2712.

[27] H. Niessen, H. Harz, P. Bedner, K. Kramer, K. Willecke, Selective permeability of different connexin channels to the second messenger inositol 1,4,5-trisphosphate, J. Cell Sci. 113 (2000) 1365-1372.

[28] J. Sneyd, B.T.R. Wetton, A.C. Charles, M.J. Sanderson, Intercellular calcium waves, mediated by diffusion of inositol (1,4,5)-trisphosphate: a two dimensional model, Am. J. Physiol. 268 (1995) C1537-C1545.

[29] T. Hoefer, L. Venance, C. Giaume, Control and plasticity of intercellular calcium waves in astrocytes: a modeling approach, J. Neurosc. 22 (12) (2002) 4850-4859.

[30] A. Goldbeter, G. Dupont, M.J. Berridge, Minimal model for signal-induced Ca^{2+} oscillations and for their frequency encoding through protein phosphorylation, Proc. Natl. Acad. Sci. USA 87 (1990) 1461-1465.

Figure Captions

Fig. 1. Behavior of function $\gamma_{ij} = \frac{k_{ij}^n}{Ca_{cytMax(ij)}^n + k_G^n}$ for different values of the power n. Here $k_{ij} = 1$ μM at $n = 5$, $k_{ij} = 1.84$ μM at $n = 3$ and $k_{ij} = 3.94$ μM at $n = 2$. We represent γ_{ij} in percentile form, or in other words normalize γ_{ij} by $max(\gamma_{ij})$ to obtain the percentile value of γ_{ij} from its maximum. For other parameters see Table 1.

Fig. 2. Different structures of connections between three cells. The grey color of cell 1 means that this cell is stimulated. The right side shows graphs that correspond to each configuration.

Fig. 3. Different structures of connections between four cells. The grey color of cell 1 means that this cell is stimulated. The right side shows graphs that correspond to each cell configuration.

Fig. 4. Intercellular calcium signaling between two cells based on diffusion of IP_3 through gap junctions. Gap junctional conductance depends on cytosolic Ca^{2+}. For all parameters see Table 1.

Fig. 5. The dependence of the time delay between initiation of oscillations in the first (stimulated) and the second cells on the amplitude of the initial impulse of IP_3 in the first cell.

Fig. 6. Intercellular calcium signaling between four cells of configurations "C", "D" and "H" (Fig. 3 C, D and H) based on diffusion of IP_3 through gap junctions. Gap junctional conductance depends on cytosolic Ca^{2+}. For all parameters see Table 1.

Fig. 7. Axis X: all configurations for four cells are separated into four different categories, taking into account the number of neighbors (see text for details). Axis Y: the mean frequency of oscillation for all cells of each configuration (mean frequency = $\frac{\text{total number}}{\text{total duration}}$ of all oscillations) with $\gamma_{ij}(Ca_{cyt})$.

Fig. 8. Intercellular calcium signaling between four cells of configuration "I" (Fig. 3 I) based on diffusion of IP_3 through gap junctions. Gap junctional conductance depends on cytosolic Ca^{2+}. For all parameters see Table 1.

Fig. 9. Intercellular calcium signaling between four cells of configuration "I" (Fig. 3 I) based on diffusion of IP_3 through gap junctions. Gap junctional conductance does not depend on cytosolic Ca^{2+}. For all parameters see Table 1.

Fig. 10. Axis X: all configurations for four cells are separated into four different categories, taking into account the number of neighbors (see text for details). Axis Y: the mean frequency of oscillation for all cells of each configuration

(mean frequency $= \frac{\text{total number}}{\text{total duration}}$ of all oscillations) with $\gamma_{ij} = 1$.

Table 1
Model parameters

Designation	Parameter values
k_{in}	1 $\mu\mathrm{M} \cdot \mathrm{s}^{-1}$
k_{out}	6 s^{-1}
k_{inIP_3}	1 s^{-1}
k_{pool}	1 s^{-1}
k_{rel}	500 $\mu\mathrm{M} \cdot \mathrm{s}^{-1}$
k_{serca}	65 $\mu\mathrm{M} \cdot \mathrm{s}^{-1}$
K_1	2 μM
K_2	0.9 μM
K_3	1 μM
V_p	0.01 s^{-1}
k_p	1 μM
k_{ij}	1 μM
k_G	0.4 μM
k_{gap}	0.005 s^{-1}

Table 2
Duration of Ca^{2+} oscillations (s)

Configuration	Cell 1	Cell 2	Cell 3	Cell 4	Total
A	11	8	8	8	35
B	11	8	8	8	35
C	12	8	6	6	32
D	12	9	8	7	36
E	10.5	7.5	7.5	7.5	37.5
F	10.5	7.5	7.5	7.5	37.5
G	11.5	8	7	7	33.5
H	10.5	7.5	7.5	8	33.5
I	11.5	9	3.5	–	24
J	12	10	8.5	7	37.5

Table 3
Time delay from the beginning of Ca^{2+} oscillations in the first cell (s)

Configuration	Cell 2	Cell 3	Cell 4
A	2.5	2.5	4
B	2	2	2
C	5	8	8
D	2	2.5	5
E	2	2	2
F	2	2	2
G	4.5	7	7
H	2.5	2.5	4
I	3.5	9.5	–
J	2	3	6

Table 4
The number of Ca^{2+} oscillations (items)

Configuration	Cell 1	Cell 2	Cell 3	Cell 4	Total
A	7	4	4	4	19
B	6	4	4	4	18
C	11	4	3	3	21
D	8	5	4	3	20
E	6	4	4	4	18
F	6	4	4	4	18
G	11	4	3	3	21
H	7	4	4	4	19
I	12	5	2	–	19
J	8	6	4	3	21

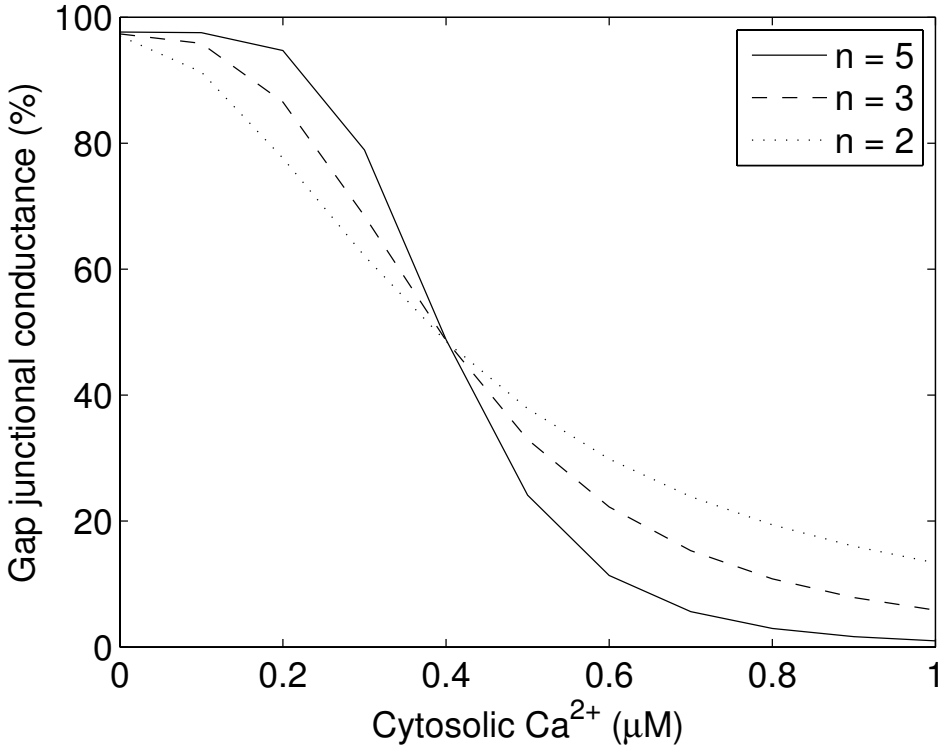
100
80
60
40
20
0
0
0.2
0.4
0.6
0.8
1
Gap junctional conductance (%)
Cytosolic Ca2+ (μM)
n = 5
n = 3
n = 2

Figure 1.

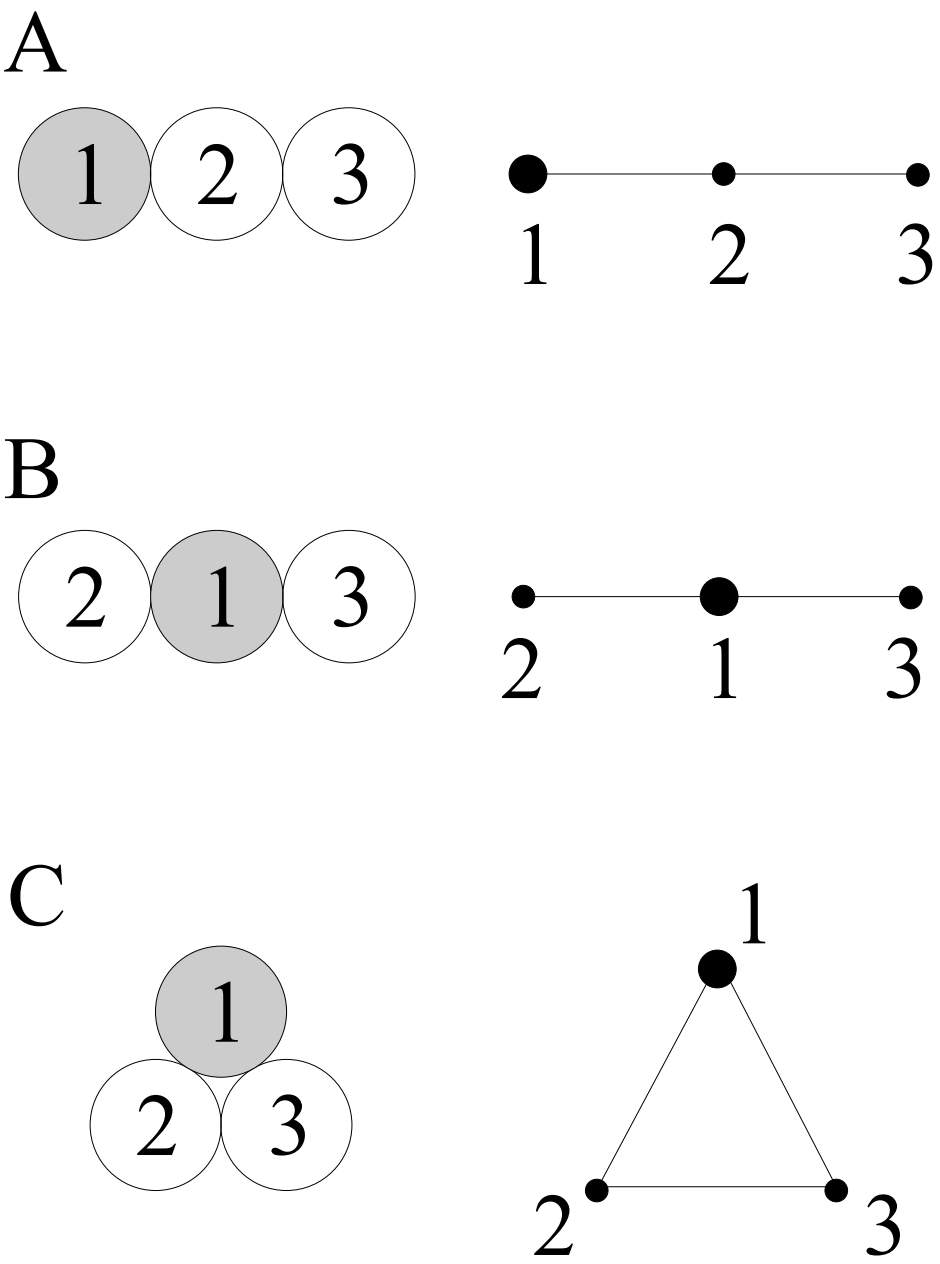

Figure 2.

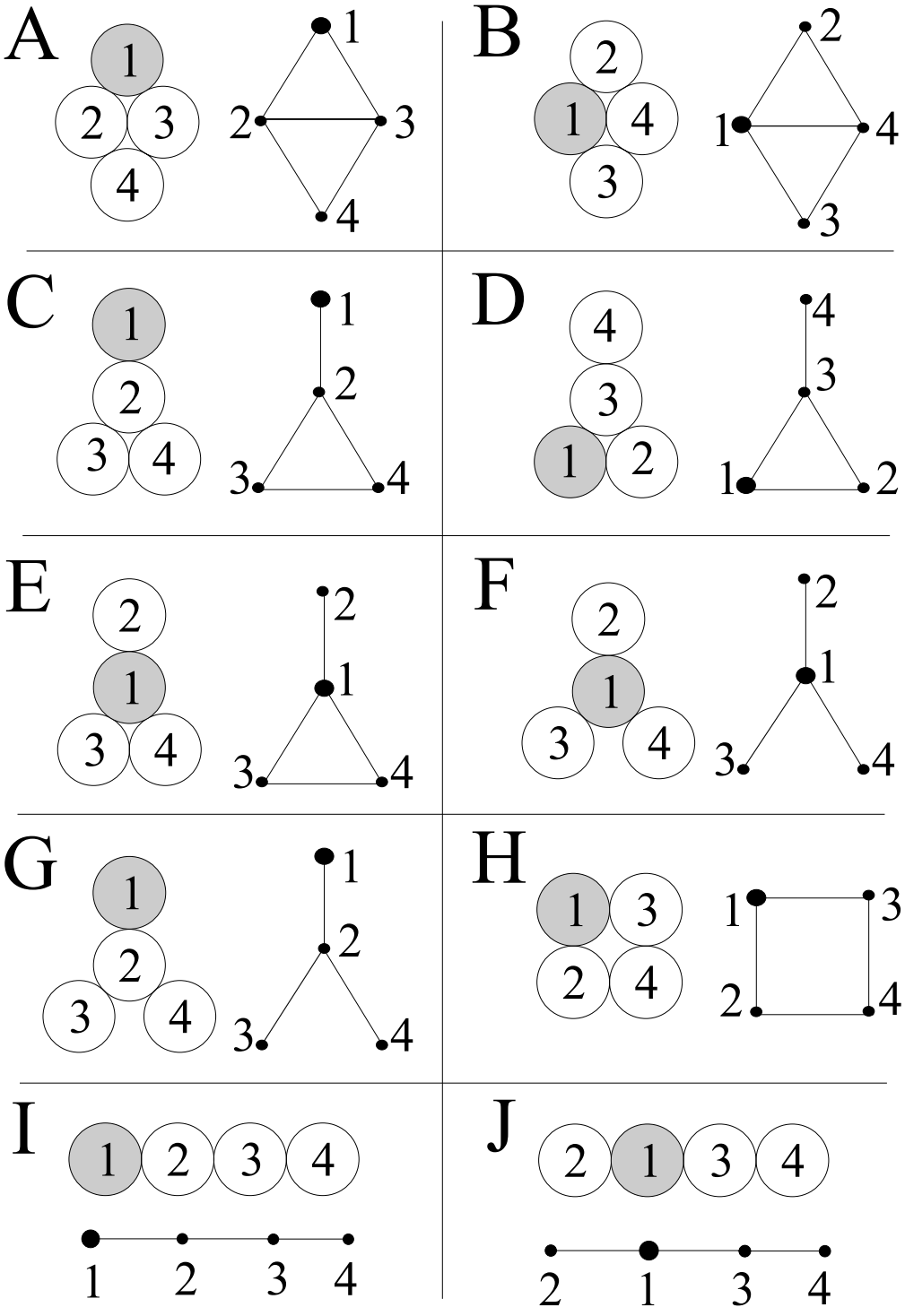
A
1
2
3
4
1
2
3
4
B
2
1
4
3
2
1
4
3
C
1
2
3
4
1
2
3
4
D
4
3
1
2
4
3
1
2
E
2
1
3
4
2
1
3
4
F
2
1
3
4
2
1
3
4
G
1
2
3
4
1
2
3
4
H
1
3
2
4
1
3
2
4
I
1
2
3
4
1
2
3
4
J
2
1
3
4
2
1
3
4

Figure 3.

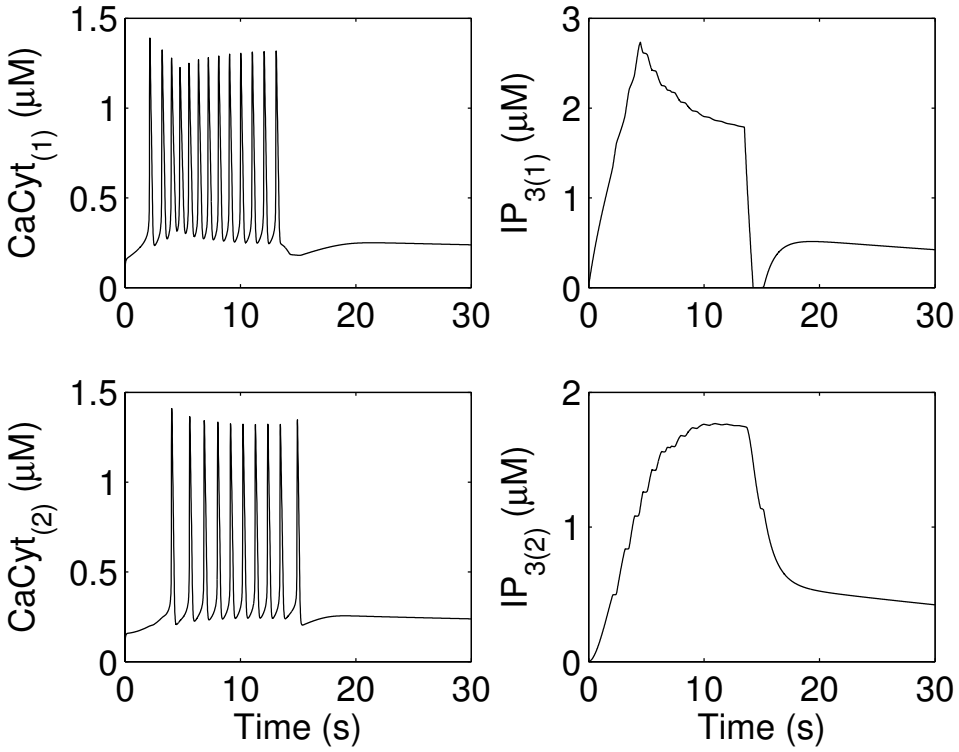

Figure 4.

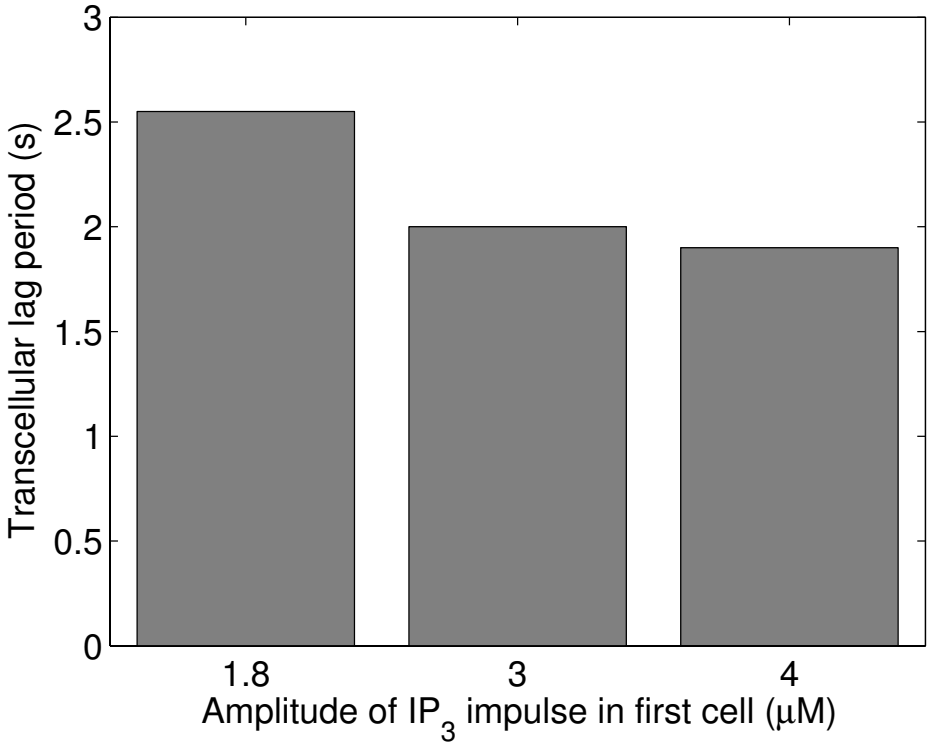
3
2.5
2
1.5
1
0.5
0
Transcellular lag period (s)
1.8
3
4
Amplitude of IP3 impulse in first cell (μM)

Figure 5.

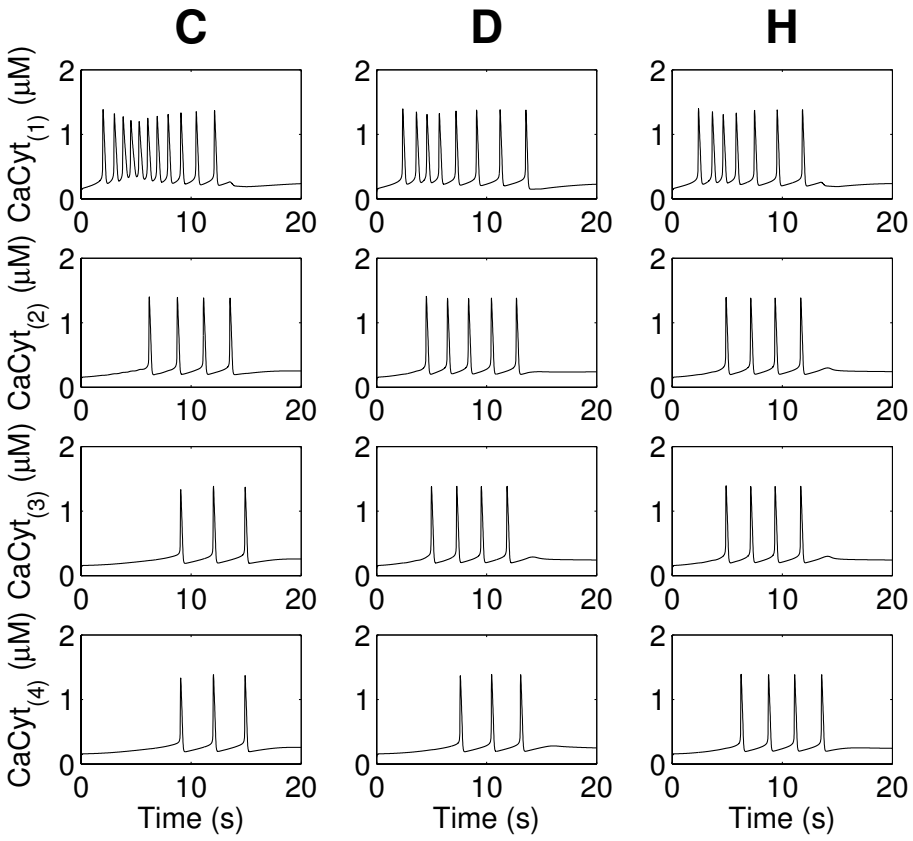
C
D
H
CaCyt(1) (μM)
CaCyt(2) (μM)
CaCyt(3) (μM)
CaCyt(4) (μM)
Time (s)
Time (s)
Time (s)

Figure 6.

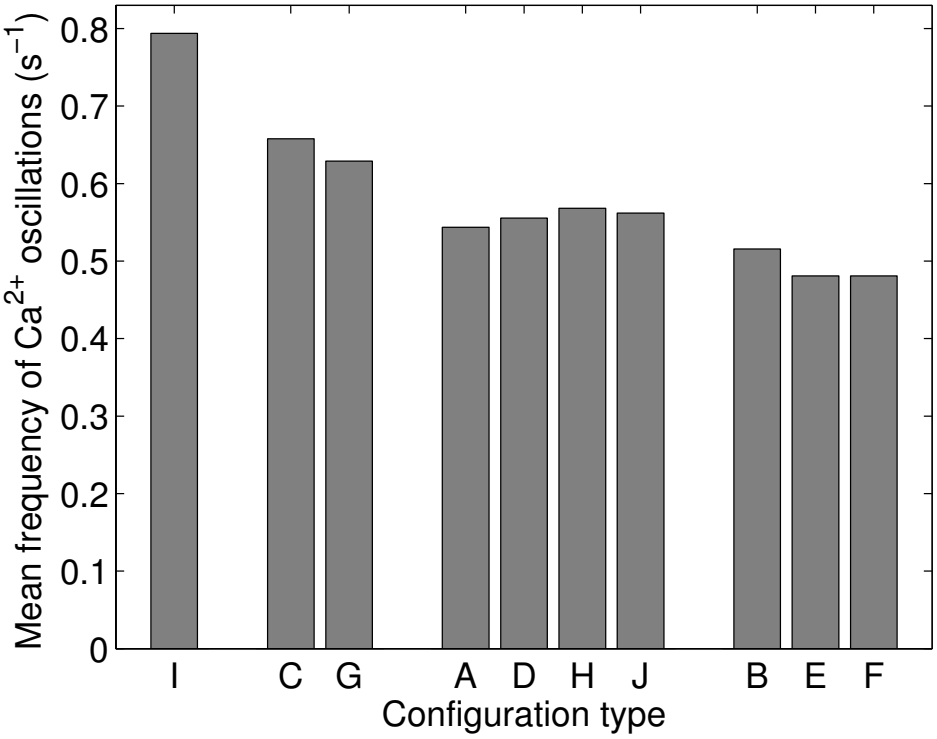
Mean frequency of Ca^{2+} oscillations (s^{-1})
0
0.1
0.2
0.3
0.4
0.5
0.6
0.7
0.8
I
C
G
A
D
H
J
B
E
F
Configuration type

Figure 7.

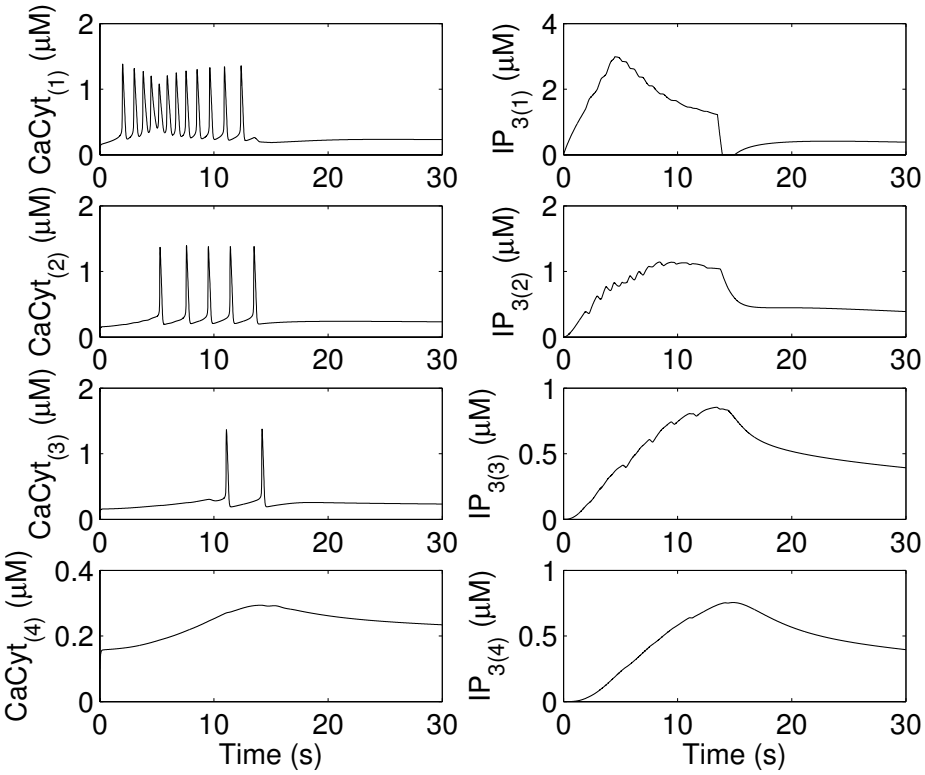
CaCyt(1) (μM)
CaCyt(2) (μM)
CaCyt(3) (μM)
CaCyt(4) (μM)
IP3(1) (μM)
IP3(2) (μM)
IP3(3) (μM)
IP3(4) (μM)
Time (s)
Time (s)

Figure 8.

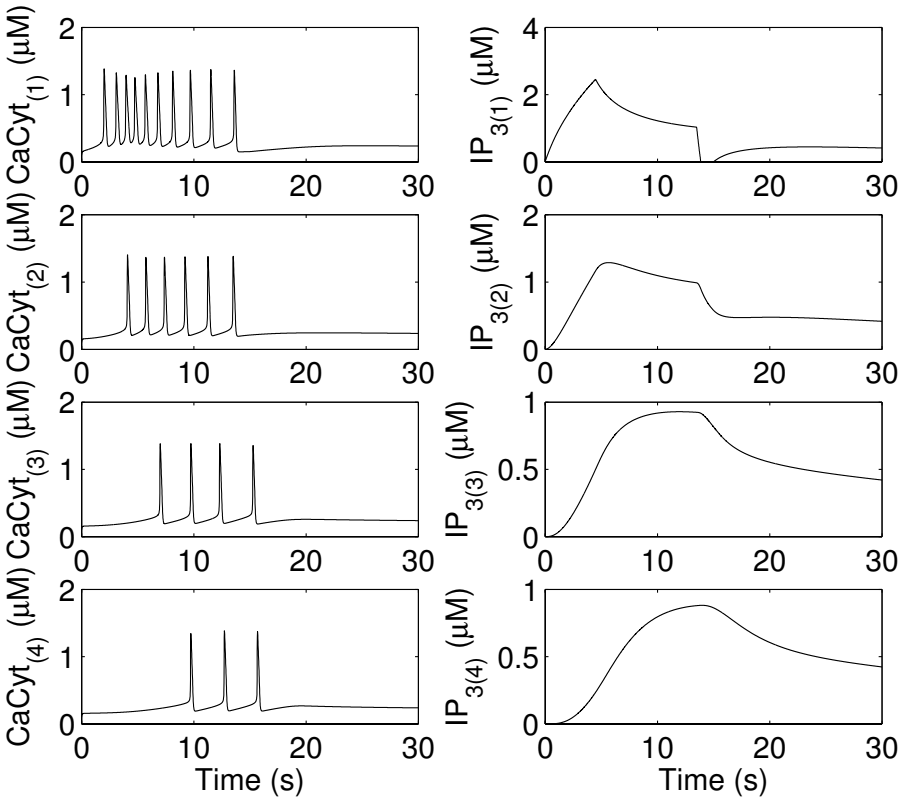
CaCyt(1) (μM)
CaCyt(2) (μM)
CaCyt(3) (μM)
CaCyt(4) (μM)
IP3(1) (μM)
IP3(2) (μM)
IP3(3) (μM)
IP3(4) (μM)
Time (s)
Time (s)

Figure 9.

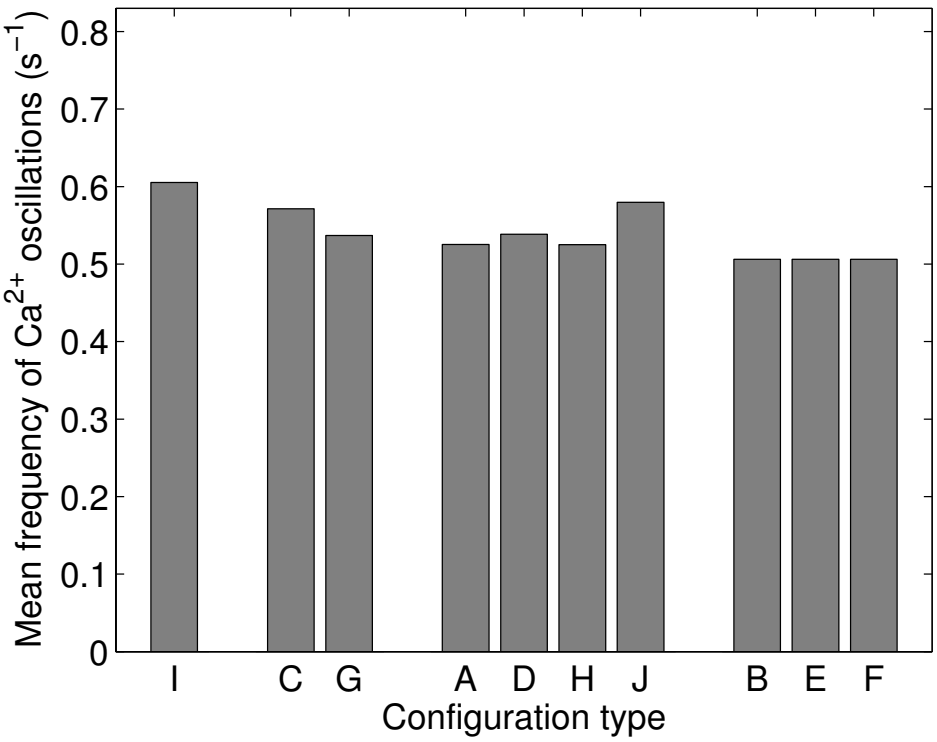
Mean frequency of Ca2+ oscillations (s−1)
0
0.1
0.2
0.3
0.4
0.5
0.6
0.7
0.8
I
C
G
A
D
H
J
B
E
F
Configuration type

Figure 10.